

## Determination of Accurate $^1\text{H}$ Positions of (Ala-Gly) $_n$ as a Sequential Peptide Model of *Bombyx mori* Silk Fibroin before Spinning (Silk I)

Tetsuo Asakura,<sup>\*,†,‡</sup> Yu Suzuki,<sup>†</sup> Koji Yazawa,<sup>†,§</sup> Akihiro Aoki,<sup>†</sup> Yusuke Nishiyama,<sup>§</sup> Katsuyuki Nishimura,<sup>‡</sup> Furitsu Suzuki,<sup>⊥</sup> and Hironori Kaji<sup>⊥</sup>

<sup>†</sup>Department of Biotechnology, Tokyo University of Agriculture and Technology, 2-24-16 Koganei, Tokyo, Japan

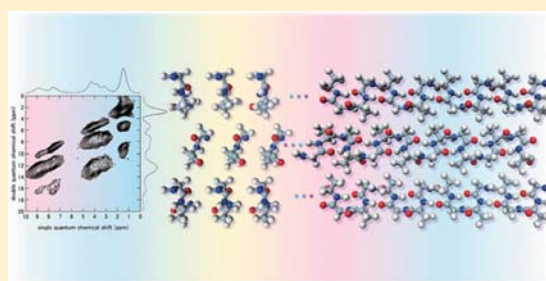
<sup>‡</sup>Institute for Molecular Science, 38 Nishigo-Naka, Myodaiji, Okazaki 444-8585, Japan

<sup>§</sup>JEOL RESONANCE Inc., 3-1-2 Musashino, Akishima, Tokyo 196-8558, Japan

<sup>⊥</sup>Institute for Chemical Research, Kyoto University, Uji, Kyoto 611-0011, Japan

### Supporting Information

**ABSTRACT:** The accurate  $^1\text{H}$  positions of alanine-glycine alternating copolypeptide, (AG) $_{15}$  with Silk I structure were determined. For the purpose, the geometry optimization was performed starting with the atomic coordinates of the hetero atoms reported previously (*Macromolecules* 2005, 38, 7397–7403) and applied only for protons under periodic boundary conditions. The agreement between the calculated and observed chemical shifts of all  $^1\text{H}$ ,  $^{13}\text{C}$  and  $^{15}\text{N}$  nuclei was excellent, indicating strongly that the determination of all the atomic-coordinate including  $^1\text{H}$  nuclei was performed with high accuracy. Here the  $^1\text{H}$  chemical shift was obtained by using both 1 mm microcoil MAS NMR probe-head for mass-limited solid-state samples developed by us and ultrahigh field NMR at 920 MHz. The DQ correlations in the  $^1\text{H}$  DQMAS NMR spectra were also used to confirm the intra- and intermolecular structures obtained here. The characteristic structure of Silk I which can be easily converted to Silk II by external forces was discussed together with the generation of Silk I structure from the aqueous solution of the silk fibroin.



## INTRODUCTION

Recently, considerable attention has been paid to *Bombyx mori* silk fibroin by a range of scientists from polymer chemists to biomedical researchers because it has excellent mechanical properties, such as strength, toughness, and biocompatibility.<sup>1</sup> These appealing physical properties originate from the silk structure, and structural analysis is therefore key to the further development of silk in biomaterial applications.

It is well-known that there are two forms of *B. mori* silk fibroin, Silk I and Silk II.<sup>1</sup> The former is the structure before spinning and the latter the structure after spinning in the solid state. Silk II was reported by Marsh et al.<sup>2</sup> to consist of anti-parallel  $\beta$ -sheet structure on the basis of the X-ray diffraction data of silk fiber. In contrast, through a combination of several solid-state NMR experiments, we proposed the conformation of Silk I model to comprise a repeated type II  $\beta$ -turn structure.<sup>3</sup> In addition, complementary information was obtained on the intermolecular arrangement of the Silk I structure through the use of X-ray powder pattern spectra.<sup>4</sup> Thus, we knew the coordinates of hetero atoms such as C, N, and O atoms. However, the coordinate of H atoms was uncertain. The H atoms are located on the surface of the silk molecule and therefore sensitive to the intermolecular arrangement in the solid state. In addition, because the generation of higher order structure and structural transition of the silk fibroin is sensitive to the breaking and formation of hydrogen bonding, it seems very

important to determine the position of the H atom such as NH which is contributed to the hydrogen bonding directly. However  $^1\text{H}$  NMR spectra in the solid state were very broad because of strong dipolar coupling. Recently, many works about high resolution  $^1\text{H}$  double-quantum (DQ) solid-state NMR of hydrogen-bonded systems and combining experiment with the gauge-including projector augmented wave (GIPAW) calculation for organic solids have been reported since the pioneer work by Spiess group from 1998.<sup>5–16</sup> We have developed a 1 mm microcoil MAS NMR probe-head for sample-limited solid-state samples.<sup>17</sup> With the combined use of such a microcoil probe-head and ultrahigh field NMR together with the geometry optimization by CASTEP and the GIPAW chemical shift calculation, we have determined the accurate  $^1\text{H}$  positions of small peptide molecules; such as alanine tripeptide and tetrapeptide with  $\beta$ -sheet structures.<sup>18,19</sup>

In this note, we report accurate  $^1\text{H}$  positions of the model peptide (Ala-Gly) $_{15}$  with Silk I structure including the verification of the coordinates of the hetero atoms such as C, N, and O reported previously.<sup>4</sup> For this purpose, we have calculated all of the  $^1\text{H}$ ,  $^{13}\text{C}$ , and  $^{15}\text{N}$  chemical shifts using both atomic coordinates reported previously<sup>4</sup> for the hetero atoms and new

**Received:** July 23, 2013

**Revised:** September 3, 2013

**Published:** September 18, 2013

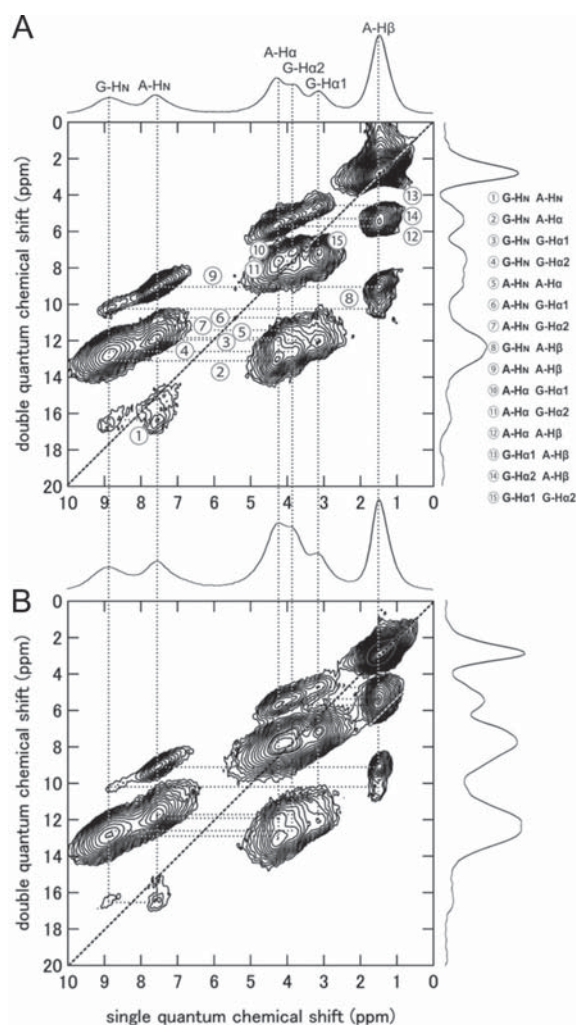


**Figure 1.** 2D  $^1\text{H}$  (920 MHz) DQMAS NMR spectra and their skyline projections of (A)  $(\text{Ala-Gly})_{15}$  and (B) Cp fraction with Silk I forms together with assignments. The DQ correlations 1–15 (circled) are shown on the right side in the spectrum A.

coordinate of  $^1\text{H}$  nuclei, and compared them with the observed chemical shifts. The observed  $^1\text{H}$  chemical shifts have been obtained by using both 1-mm microcoil MAS NMR probe-head for sample-limited solid-state analysis and ultrahigh field NMR at 920 MHz. The DQ correlations in the  $^1\text{H}$  DQMAS (double quantum magic angle sequence) NMR spectra have also been used to confirm the intra- and intermolecular structures of  $(\text{Ala-Gly})_{15}$  with Silk I structure obtained here.

## EXPERIMENTAL SECTION

**NMR Observation.** As the crystalline fraction of the silk fibroin, the precipitate fraction (Cp fraction) was prepared via the chymotrypsin reaction of *B. mori* silk fibroin in the Silk I form, as described previously.<sup>3</sup>  $(\text{Ala-Gly})_{15}$  with Silk I form was synthesized by the solid phase method. The  $^1\text{H}$  solid state DQMAS experiment was performed at a  $^1\text{H}$  resonance frequency of 920 MHz using a JEOL JNM-ECA920 spectrometer equipped with  $^1\text{H}$ -X double resonance and 1 mm ultrahigh speed MAS probe at the Institute for Molecular Science (IMS) in Okazaki, Japan. The sample amount is ca. 0.8 mg. The sample spinning speed was actively stabilized by a pneumatic solenoid valve so that the spinning fluctuations were less than  $\pm 10$  Hz at a spinning rate of 70 kHz. The temperature of the samples increases due to friction effect of the fast MAS and is estimated 333 K at 70kHz MAS by  $\text{Pb}(\text{NO}_3)_2$

**Table 1.** Calculated ( $\delta_{\text{calc}}$ ) and Observed ( $\delta_{\text{obs}}$ )  $^1\text{H}$ ,  $^{13}\text{C}$ , and  $^{15}\text{N}$  Chemical Shifts (in ppm) of  $(\text{Ala-Gly})_{15}$  with Silk I Structure in the Solid State<sup>a</sup>

	G-C $\alpha$	G-CO	A-C $\alpha$	A-C $\beta$	A-CO
$\delta_{\text{calc}}$	45.1	168.0	52.1	18.9	175.3
$\delta_{\text{obs}}$	43.8	170.7	51.4	16.5	177.0
$\delta_{\text{obs-a}}$	42.7	171-172	50.0	16.6	175-176

	G-H $_N$	G-H $\alpha$ 1	G-H $\alpha$ 2	A-H $_N$	A-H $\alpha$	A-H $\beta$
$\delta_{\text{calc}}$	9.1	3.5	2.9	8.3	4.1	1.2
$\delta_{\text{obs}}$	8.8	3.8	3.1	7.6	4.3	1.5
$\delta_{\text{obs-a}}$	8.3-8.5	3.7-3.9		8.2-8.4	4.2-4.3	1.3-1.4

	G-N	A-N
$\delta_{\text{calc}}$	88.6	102.3
$\delta_{\text{obs}}$	88.1	102.7
$\delta_{\text{obs-a}}$	88	103

<sup>a</sup>The reference chemical shift in the calculated value was chosen such that the mean of the calculated and observed chemical shifts for all peaks.<sup>7,9</sup> The reference chemical shift values were 30.51 ppm, 171.31 ppm, and 197.22 ppm for  $^1\text{H}$ ,  $^{13}\text{C}$ , and  $^{15}\text{N}$  nuclei, respectively. The observed  $^1\text{H}$ ,  $^{13}\text{C}$ , and  $^{15}\text{N}$  chemical shifts ( $\delta_{\text{obs-a}}$ ) of the aqueous solution of *B. mori* silk fibroin are also listed.

temperature calibration. For  $^1\text{H}$  DQMAS, Dipolar Homonuclear Homogeneous Hamiltonian double-quantum/single-quantum correlation measurement ( $\text{DH}_3\text{DQ-SQ}$ ) was employed.<sup>20</sup> The spectral width of indirect dimension was set to 200kHz, 64  $t_1$  increments with 32 transients each were recorded with a 2 s recycle delay. The  $2\tau$  delay was optimized to 0.3 ms, thereby giving maximum S/N. The  $^1\text{H}$  nutation frequency for recoupling was 192 kHz. The  $90^\circ$  pulse length was 1.29  $\mu\text{s}$ . Phase sensitive detection in the indirect dimension was obtained using the States method.<sup>21</sup> The  $^1\text{H}$  chemical shift was referenced to the peak of silicon rubber and set to 0.12 ppm from TMS.

**Chemical Shift Calculation.** In our previous paper,<sup>5</sup> we reported the atomic level structure of  $(\text{AG})_{15}$  with Silk I structure as follows. The unit cell and space group was orthorhombic and  $P2_12_12_1$ , respectively. The lattice constants were  $a = 4.65 \text{ \AA}$ ,  $b = 14.24 \text{ \AA}$ , and  $c = 8.88 \text{ \AA}$ ,  $\alpha = \beta = \gamma = 90^\circ$ . There are four repeated units, Ala-Gly, in a unit cell. Two  $2_1$ -helix chains are included with antiparallel forms in a unit cell. The torsion angles  $(\phi, \varphi) = (-62^\circ, 125^\circ)$  for Ala residue and  $(\phi, \varphi) = (77^\circ, 10^\circ)$  for Gly residue of poly(Ala-Gly) chain.

In this work, we fixed the atomic coordinates of the hetero atoms. Then the geometry optimization was applied only for protons under periodic boundary conditions. The generalized gradient approximation (GGA) for the exchange correlation energy using the Perdew, Bruke, and Ernzerhof (PBE) functional and ultrasoft pseudopotentials with a plane-wave energy cutoff of 27.9 Ry (380 eV) was used for such a geometry optimization. A  $5 \times 2 \times 3$  Monkhorst-Pack  $k$ -point grid was used for Brillouin zone sampling for all the above crystal structures. All calculations were carried out by the NMR-CASTEP program. The  $^1\text{H}$ ,  $^{13}\text{C}$ , and  $^{15}\text{N}$  chemical shift calculations were then performed by GIPAW methods. The PBE approximation and “on the fly” pseudopotentials were used. The energy cutoff of the plane wave was set to 44.8 Ry (610 eV). A  $5 \times 2 \times 3$  Monkhorst-Pack  $k$ -point grid was used for Brillouin zone sampling for all the structures. The reference chemical shift of the calculated chemical shifts was determined to

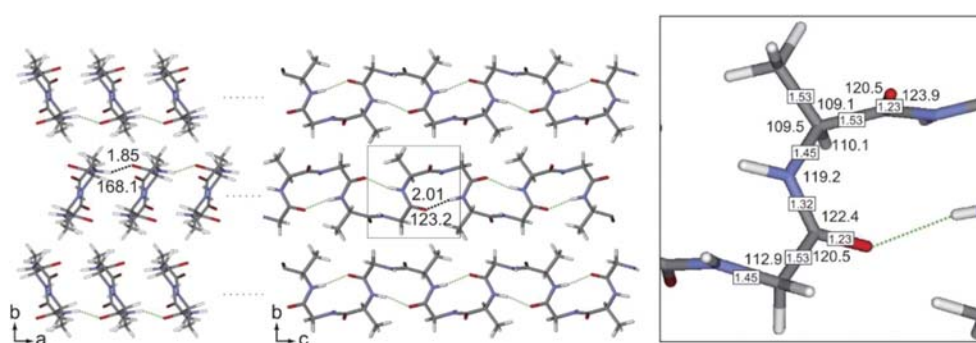
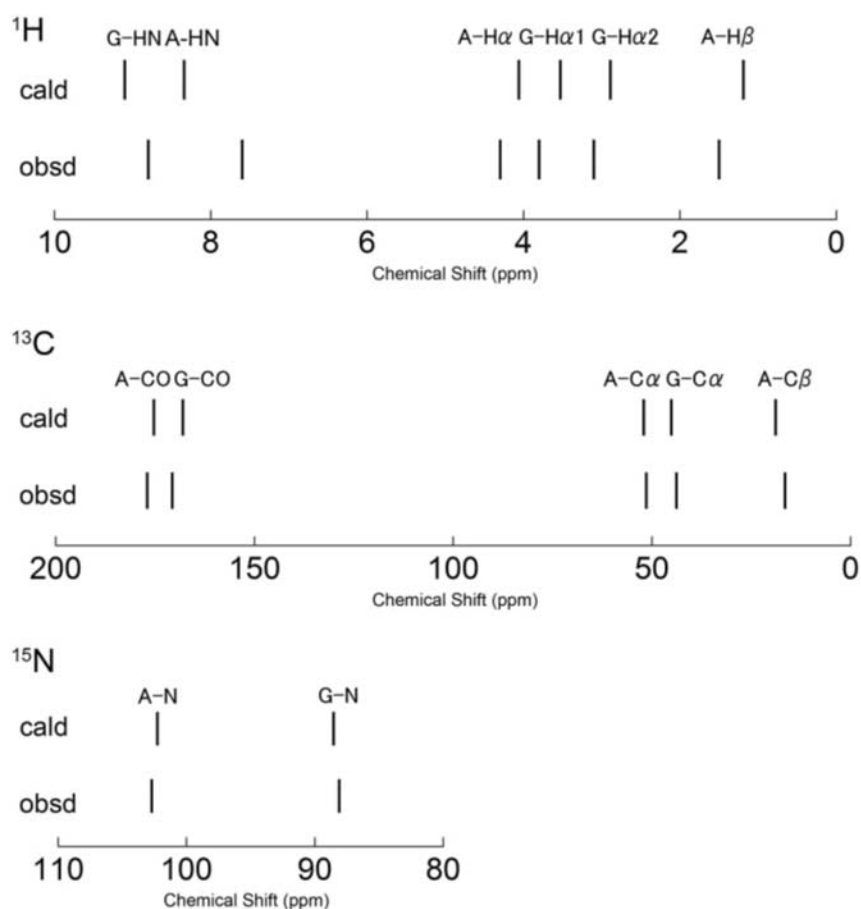


**Figure 2.** The stick spectra for the  $^1\text{H}$ ,  $^{13}\text{C}$ , and  $^{15}\text{N}$  chemical shifts calculated for  $(\text{Ala-Gly})_{15}$  with Silk I structure together with the observed chemical shifts. Further calculated results are listed in Table 1S in the Supporting Information. The reference chemical shift was shown to be the mean of the calculated and observed chemical shifts for all peaks.<sup>7,9</sup> The values were 30.51, 171.31, and 197.22 ppm for  $^1\text{H}$ ,  $^{13}\text{C}$ , and  $^{15}\text{N}$  nuclei, respectively. The structure after CASTEP calculation was also shown. The distance (upper value), and angle (lower value) between NH and CO bonds which contribute to the direct hydrogen bonding formation in intermolecular hydrogen bonding was shown in the left side. Those in intramolecular hydrogen bonding was shown in the center. The bond lengths (The values in the square) and bond angles were shown in the right side.

minimize the difference between the observed and calculated chemical shifts without changing the relative chemical shift difference among every peaks.<sup>9</sup> The values were 30.51, 171.31, and 197.22 ppm for  $^1\text{H}$ ,  $^{13}\text{C}$ , and  $^{15}\text{N}$  nuclei, respectively.

## RESULTS AND DISCUSSION

Figure 1 shows 2D  $^1\text{H}$  DQMAS spectra and their skyline projections of A:  $(\text{Ala-Gly})_{15}$  and B: Cp fraction with Silk I

forms. The spectra are very similar between  $(\text{Ala-Gly})_{15}$  and Cp fraction. For example, the dashed vertical lines that the hydrogen-bonded NH chemical shifts have the same centers of gravity. Because of the presence of Ser residue in Cp fraction, the  $\text{H}\alpha$  region is slightly broader due to the presence of the Ser peaks. Thus, only the data of  $(\text{Ala-Gly})_{15}$  in the Silk I form are discussed below. The observed chemical shifts are listed in

Table 1 together with those of  $^{13}\text{C}$  and  $^{15}\text{N}$  chemical shifts of  $(\text{Ala-Gly})_{15}$  with Silk I structure, and also the chemical shifts of the aqueous solution of *B. mori* silk fibroin.<sup>22,23</sup> It is noted that the Gly methylene peak splits into two peaks Gly-H $\alpha_1$ , Gly-H $\alpha_2$  with the chemical shift difference, 0.7 ppm, indicating that electrostatic environment is considerably different between these two protons in the solid state. On the other hand, the two methylene peaks of Gly residue of *B. mori* silk fibroin in aqueous solution have the same chemical shift and close to the chemical shift, Gly-H $\alpha_1$  rather than Gly-H $\alpha_2$  in the solid state. In addition, the Gly-HN peak move to lower field by 0.3–0.5 ppm, while Ala-HN peak to higher field by 0.6–0.8 ppm in the solid state relative to the Gly- and Ala-HN chemical shifts of the silk fibroin in aqueous solution. This difference reflects the difference in the structures between Silk I in the solid state and random coil in the aqueous solution.

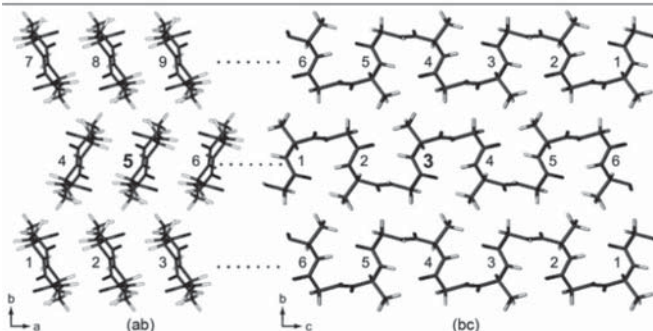
The geometry optimization was applied only for protons under periodic boundary conditions after the atomic coordinates of the hetero atoms were fixed. The calculated chemical shifts are listed in Table 1. More detailed results of the chemical shift calculation are listed (Table 1S: Supporting

Information). Figure 2 shows the stick spectra of the  $^1\text{H}$ ,  $^{13}\text{C}$ , and  $^{15}\text{N}$  chemical shifts calculated for  $(\text{Ala-Gly})_{15}$  in the Silk I form together with the observed chemical shifts in order to facilitate comparison. The agreement between the calculated and observed chemical shifts is excellent for all  $^1\text{H}$ ,  $^{13}\text{C}$ , and  $^{15}\text{N}$  nuclei as reported for the combining experiment of  $^1\text{H}$  DQ NMR with the GIPAW calculation for organic solids.<sup>7,14,16</sup> A better agreement between the calculated and experimental data is expected for hydrogen-bonded amide protons by comparing to an extrapolated observed chemical shift at 0 K.<sup>14</sup> Thus, these results suggest strongly that the coordinates of  $(\text{Ala-Gly})_{15}$  in the Silk I form after CASTEP calculation can be determined with a high degree of accuracy. In particular, the structure determination methods for  $^{13}\text{C}$  and  $^{15}\text{N}$  positions of Silk I reported previously,<sup>4</sup> the  $^1\text{H}$  optimization method performed in this work and the  $^1\text{H}$ ,  $^{13}\text{C}$ , and  $^{15}\text{N}$  chemical shift calculations with GIPAW method are all valid.

As shown in Figure 1, 15 DQ correlations were observed although some of the DQ pair could not be observed clearly because of the overlap in the other DQ correlations. Although we did not attempt the observation of  $^1\text{H}$  DQ build-up and the

**Table 2.** Intra- and Inter-Molecular  $^1\text{H}$ – $^1\text{H}$  Distances (in Å) of  $(\text{Ala-Gly})_{15}$  in the Silk I Form Calculated from the New Co-Ordinates Obtained from the CASTEP Calculation in This Work<sup>a</sup>

DQ correlation		Intra-molecular		Inter-molecular	
①	G-HN A-HN	2.83	(5 3)	3.43	(4 3)
②	G-HN A-H $\alpha$	2.12	(5 2)	3.46	(4 3)
③	G-HN G-H $\alpha_1$	2.30	(5 3)		
④	G-HN G-H $\alpha_2$	2.88	(5 3)	2.76, 3.42	(2 5),(4 3)
⑤	A-HN A-H $\alpha$	2.86, 3.52	(5 3),(5 2)	2.96	(4 3)
⑥	A-HN G-H $\alpha_1$	3.28, 3.99	(5 3),(5 2)		
⑦	A-HN G-H $\alpha_2$	3.47	(5 3)		
⑧	G-HN A-H $\beta$	3.89	(5 2)		
⑨	A-HN A-H $\beta$	2.87	(5 3)		
⑩	A-H $\alpha$ G-H $\alpha_1$			3.23	(6 3)
⑪	A-H $\alpha$ G-H $\alpha_2$			3.66	(9 4)
⑫	A-H $\alpha$ A-H $\beta$	2.70	(5 3)		
⑬	G-H $\alpha_1$ A-H $\beta$	3.65	(5 4)	3.56	(2 4)
⑭	G-H $\alpha_2$ A-H $\beta$			3.60	(3 4)
⑮	G-H $\alpha_1$ G-H $\alpha_2$	1.77	(5 3)		



<sup>a</sup>For example, 1 (circled) G–H<sub>N</sub> A–H<sub>N</sub> 2.83 (5 3) means that the atomic distance is 2.83 Å between H<sub>N</sub> Gly and H<sub>N</sub> Ala in the chain number 5 in the group (ab) and the number of Ala-Gly segment 3 in the group (bc). The number of the DQ correlations 1–15 is the same as those circled in Figure 1.

quantitative simulation, we tried to understand qualitatively the relationship between the observed DQ correlation and relative proton–proton proximities from the coordinates of (Ala-Gly)<sub>15</sub> with Silk I form. Actually, the detailed analysis of the DQ correlations showed that the relative DQ peak intensities are a reliable measure of the relative distances.<sup>12,16</sup> The intramolecular and intermolecular <sup>1</sup>H–<sup>1</sup>H distances less than 4 Å were calculated from the coordinates and listed in Table 2. Thus, all of the <sup>1</sup>H–<sup>1</sup>H distances predicted were observed in the <sup>1</sup>H DQMAS spectrum (Figure 1).

The geometry of the hydrogen bonding arrangements is revealed by the geometry-optimized Silk I structure. The intramolecular hydrogen bonding distance was 2.01 Å between the NH of the (*i* + 3)-th Ala residue and CO of *i*-th Gly residue and the intermolecular hydrogen bonding distance was 1.85 Å between the NH of the (*i* + 2)-th Gly residue in one chain and CO of the (*i* + 1)-th Ala residue in another chain. The angles between NH and CO bonds which contribute to the direct hydrogen bonding formation are 123.2° and 168.1°, respectively. Especially, the angle, 123.2° is far from the preferred linearity for a hydrogen bond. Thus, judging from both the distance and angle of hydrogen bonding, the intermolecular hydrogen bonding in Silk I structure is considerably stronger than the intramolecular hydrogen bonding. The plane of the NH–CO peptide and the intra- and intermolecular hydrogen bonding appears alternatively and is perpendicular to each other. Thus, it may be speculated that intramolecular hydrogen bonding is easily destroyed by external forces such as stretching. The coordinate of Silk I obtained here will be a key to clarify the mechanism of the formation of *B. mori* silk fiber with excellent physical properties more quantitatively.

## ■ ASSOCIATED CONTENT

### ■ Supporting Information

Calculated <sup>1</sup>H, <sup>13</sup>C, and <sup>15</sup>N chemical shifts. This material is available free of charge via the Internet at <http://pubs.acs.org>.

## ■ AUTHOR INFORMATION

### Corresponding Author

\*E-mail: (T.A.) [asakura@cc.tuat.ac.jp](mailto:asakura@cc.tuat.ac.jp).

### Notes

The authors declare no competing financial interest.

## ■ ACKNOWLEDGMENTS

T.A. acknowledges support from Grant-in-Aid for Scientific Research from the Ministry of Education, Science, Culture and Supports of Japan (23245045,25620169) and the Ministry of Agriculture, Forestry and Fisheries of Japan (Agri-Health Translational Research Project). T.A. also acknowledges useful discussion with Prof. Mike Williamson, University of Sheffield, U.K.

## ■ REFERENCES

- (1) Asakura, T., Miller, T., Eds. *Biotechnology of Silk*: Springer: Berlin, 2013.
- (2) Marsh, R. E.; Corey, R. B.; Pauling, L. *Biochim. Biophys. Acta* **1955**, *16*, 1.
- (3) Asakura, T.; Ashida, J.; Yamane, T.; Kameda, T.; Nakazawa, Y.; Ohgo, K.; Komatsu, K. *J. Mol. Biol.* **2001**, *306*, 291.
- (4) Asakura, T.; Ohgo, K.; Komatsu, K.; Kanenari, M.; Okuyama, K. *Macromolecules* **2005**, *38*, 7397.
- (5) Schnell, I.; Brown, S. P.; Low, H. Y.; Ishida, H.; Spess, H. W. *J. Am. Chem. Soc.* **1998**, *120*, 11784.

- (6) Pickard, C. J.; Mauri, F. *Phys. Rev. B* **2001**, *63*, 245101.
- (7) Yates, J. R.; Pham, T. N.; Pickard, C. J.; Mauri, F.; Amado, A. M.; Gil, A. M.; Brown, S. P. *J. Am. Chem. Soc.* **2005**, *127*, 10216.
- (8) Yates, J. R.; Pickard, C. J.; Mauri, F. *Phys. Rev. B* **2007**, *76*, 024401.
- (9) Brown, S. *Prog. Nucl. Magn. Reson. Spectrosc.* **2007**, *50*, 199.
- (10) Brinkmann, A.; Litvinov, V. M.; Kentgens, A. P. M. *Magn. Reson. Chem.* **2007**, *45*, S231.
- (11) Mafra, L.; Siegel, R.; Fernandez, C.; Schneider, D.; Aussenac, F.; Rocha, J. *J. Magn. Reson.* **2009**, *199*, 111.
- (12) Bradley, J. P.; Tripon, C.; Filip, C.; Brown, S. P. *Phys. Chem. Chem. Phys.* **2009**, *11*, 6941.
- (13) Harris, R. K.; Hodgkinson, P.; Zorin, V.; Dumez, J. N.; Herrmann, B. E.; Emsley, L.; Salager, E.; Stein, R. S. *Magn. Reson. Chem.* **2010**, *48*, S103.
- (14) Webber, A. L.; Elena, B.; Griffin, J. M.; Yates, J. R.; Pham, T. N.; Mauri, F.; Pickard, C. J.; Gil, A. M.; Stein, R.; Lesage, A.; Emsley, L.; Brown, S. P. *Phys. Chem. Chem. Phys.* **2010**, *12*, 6970.
- (15) Kins, C. F.; Dudenko, D.; Sebastiani, D.; Brunklaus, G. *Macromolecules* **2010**, *43*, 7200.
- (16) Brown, S. P. *Solid State Nucl. Magn. Reson.* **2012**, *41*, 1.
- (17) Yamauchi, K.; Yamasaki, S.; Takahashi, R.; Asakura, T. *Solid State Nucl. Magn. Reson.* **2010**, *38*, 27.
- (18) Yazawa, K.; Suzuki, F.; Nishiyama, Y.; Ohata, T.; Aoki, A.; Nishimura, K.; Kaji, H.; Shimizu, T.; Asakura, T. *Chem. Commun.* **2012**, *48*, 11199.
- (19) Asakura, T.; Yazawa, K.; Horiguchi, K.; Suzuki, F.; Nishiyama, Y.; Nishimura, K.; Kaji, H. *Biopolymers* **2013**, in press.
- (20) Deschamps, M.; Fayon, F.; Cadars, S.; Rollet, A. L.; Massiot, D. *Phys. Chem. Chem. Phys.* **2011**, *13*, 8024.
- (21) States, D. J.; Haberkorn, R. A.; Ruben, D. J. *J. Magn. Reson.* **1982**, *48*, 286.
- (22) Suzuki, Y.; Takahashi, R.; Shimizu, T.; Tansho, M.; Yamauchi, K.; Williamson, M. P.; Asakura, T. *J. Phys. Chem. B* **2009**, *113*, 9756.
- (23) Asakura, T.; Demura, M.; Date, T.; Miyashita, N.; Ogawa, K.; Williamson, M. P. *Biopolymers* **1997**, *41*, 193.